The 11th International Symposium on Virtual Reality, Archaeology and Cultural Heritage VAST (2010)
A. Artusi, M. Joly-Parvex, G. Lucet, A. Ribes, and D. Pitzalis (Editors)

GigaMesh and Gilgamesh – 3D Multiscale Integral Invariant Cuneiform Character Extraction

Hubert Mara[1], Susanne Krömker[1], Stefan Jakob[2] and Bernd Breuckmann[3]

[1]IWR – Interdisciplinary Center for Scientific Computing of the Heidelberg University, Im Neuenheimer Feld 368, 69120 Heidelberg, Germany
[2] Seminar für Sprachen und Kulturen des Vorderen Orient, Assyriologie, Heidelberg University, Hauptstr. 126, 69117 Heidelberg, Germany
[3]Breuckmann GmbH, Torenstr. 14, 88709 Meersburg, Germany

Abstract

As assyriologists have to handle tremendous amounts of important documents of ancient history written in cuneiform script, like the epic of Gilgamesh*, we are developing an efficent system to support their daily tasks. Previous projects demonstrated the application of holography and early close-range 3D scanners for this task. Based on experiences from our previous projects in archaeology, we are focusing on processing the vast amounts of data of high resolution 3D models (µm-range) from todays close-range 3D scanners like the* Breuckmann smartSCAN-3D-HE.

The presented method exploits the high-resolution of the 3D models to extract the impressed characters as well as other features like fingerprints. Previous work typically used rendering techniques from computer graphics to visualize the characters, which then had to be processed manually. More recent approaches use methods from differential geometry for detection and extraction of coarse contour lines. These methods are computationally fast, and well-established for industrial application, but cannot cover the variations of human handwriting in form of the – wedge shaped – cuneiform script. To overcome the variations in size of the wedges, we choose a multiscale approach using integrating geometry. A transformation invariant function is achieved by calculating the volumes of multiple concentric spheres intersecting the volume below the 3D model's surface at each point. Due to this multiscale approach, this function is represented by the so-called feature vector*. By classifying these* feature vectors *using auto-correlation, our system – called* GigaMesh *– can automatically extract characters, requiring only one parameter: the approximated line (wedge) width in mm.*

Results are shown for cuneiform tablets from the collections of the Assyriologie Heidelberg *as well as from the* Uruk-Warka Sammlung*. Finally an outlook regarding character (en)coding and integration into related projects like the* Cuneiform Digital Library Initiative *(CDLI) is given.*

Categories and Subject Descriptors (according to ACM CCS): I.4.6 [Image Processing and Computer Vision]: Edge and feature detection—I.7.5 [Document and Text Processing]: Optical Character Recognition (OCR)—I.3.7 [Computer Graphics]: Color, shading, shadowing, and texture—J.5 [Arts and Humanities]: Linguistics—

1. Introduction

Motivated by the demand of epigraphy to document and analyze large quantities of "writings in 3D", which are inscriptions and the handwritten cuneiform script [vS94], we are developing a highly automated system using state-of-the-art 3D technology [KMT08]. As our current main focus is on cuneiform script, which is most famous for the epic of *Gilgamesh* [Mau05], we call our system *GigaMesh* as it is meant to process the tremendously large meshed structures of high-resolution 3D scans [MBLA09] of cuneiform tablets. The traditional first step of documentation for all "writings in 3D" is done by taking photographs for cuneiform script and/or creating chalkings [MHK09] for inscriptions. Both methods are nonreversible projections on pieces of plane paper, which are used to manually copy the characters by drawing for transliteration and finally translation [NDE91, Feu00]. Being aware of the influence of the projections properties (e.g. illumination while taking the

© The Eurographics Association 2010.

DOI: 10.2312/VAST/VAST10/131-138

delivered by EUROGRAPHICS DIGITAL LIBRARY www.eg.org diglib.eg.org

photographs) to the final translation, scholars often hardcopy objects in situ by casting them into gipsum, clay or latex. These casts give them the possibility to study objects back home in the office in almost the same way as the originals, which have to stay within an excavation storage or a museum.

The fact that producing casts costs time, perhaps damages the original and the casts themselves are more fragile than the originals lead to the idea to document cuneiforms using holography [vBVD*94, WGD*98, DKK*02]. Even today, as holography is part of many objects of daily life like banknotes, the process of taking holographic images requires large and power consuming equipment, rendering this approach impracticable for assyriologists. Nevertheless, early projects had the proper foresight and added pattern recognition and image processing techniques to their approach [Ros97]. Consequently this lead to the *Digital Hammurabi* [WS03] project and the *Cuneiform Digital Forensic Project* (CDFP) [WTN*02] experimenting with various types of close range 3D scanners. Thanks to the *Initiative for Cuneiform Encoding* (ICE) [Feu00] at the same time as the CDFP, cuneiform script became part of the *Unicode* standard [Uni06]. Free *TrueType* fonts became available e.g. for LaTeX.

By present day the most active project using modern technologies in a *Web 2.0* spirit is the *Cuneiform Digital Library Initiative* (CDLI), which follows the idea of focusing more on working with the content of the tablets like the database project from *Göttingen* [GWLU05, Wei10]. This left us with a digital workflow for presenting and publishing content like [Hil08] of the *CDLJournal*, but only a sketchy workflow to replace the cast copies and photographs by new technologies.

2. Data Acquisition and Resolution

As shown in [WTN*02] and from our experience in archaeological projects, we decided to use a 3D scanner based on the principles of structured light and stereo vision [SM92]. After extensive tests of different models from different vendors, we choose a *Breuckmann smartSCAN-3D-HE*, because it features the highest spatial resolution **and** acquisition of a colored texture map using two color cameras. Color acquisition is important to match broken tablets as well as for other projects related to cultural heritage [MBLA09]. For the *smartSCAN-3D-HE* exists a wide range of different optics, which is categorized by the range image diagonal – also called *Field of View* (FOV) – and not the focal length.

For many archaeological finds the FOV of 150 mm has proven to be the best choice to acquire small details like fingerprints. When objects contain smaller details, like seal imprints and toolmarks, the FOV with 60 mm is recommended. The FOVs of 470, 600 and 1.000 mm are suitable to acquire larger objects like reliefs and statues – even whole temples [QTK*09]. For flat objects – as tablets sometimes are – a comparison with flat bed scanners can be roughly estimated in *Dots Per Inch* (*DPI*) by dividing the cardinality of the measuring points (vertices) by the acquired surface (in square inch) of the resulting 3D model. Having a 3D scanner based on 5,0 megapixels cameras we can achieve $\approx 1{,}000$ *DPI* for the FOV of 60 mm, ≈ 300 *DPI* for the FOV of 150 mm down to ≈ 100 *DPI* for the larger FOVs. Recently a FOV of 35 mm has been added for forensic sciences, which pushs the resolution up to $\approx 2{,}500$ *DPI* – equaling a spatial resolution within the 10 μm-range. Figure 1 shows the *smartSCAN-3D-HE* during acqisition using the 60 mm FOV.

A single 3D scan requires a few seconds independent of the chosen optics. For first experiments with cuneiform tablets, the whole acquisition workflow took between 5 and 45 *minutes* depending on the size of the tablet as well as the quality, condition and utilization/density of the cuneiform characters.

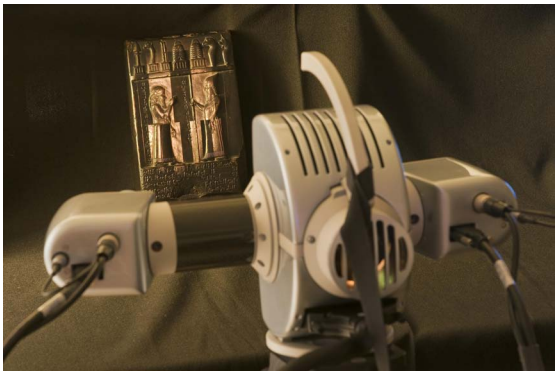

Figure 1: *Tablet Inv. No. BM 90922,* King, Boundary Stones, No. XXVIII, *acquired by a* Breuckmann smartSCAN-3D-HE *using the* 60 *mm field of view optics.*

3. Data Processing

Considering the manufacturing process of a cuneiform tablet, it is a smooth piece of clay having wedges imprinted by a stylus. This lead to a first approach, which is virtually smoothing the surface to the tablets overall shape having no small details, like an empty tablet. One expects that having a virtual empty tablet its distance [CRS01] to the measured surface will allow to segment the cunei (Latin for wedges). In this context the distance map can also be called displacement map or height map. Figure 2a shows a tablet and Figure 2b shows in different colors the distances to its smoothed surface. The coloring in Figure 2b is similar to height maps from cartography and it shows that the expectation is only partially fulfilled.

Ambient occlusion [Bun05] from computer graphics promises to shade corners darker, but the output data structure is a projected 2D raster image, which limits any further processing, as it also has low differences in contrast between wedges and the overall surface. A better approach

© The Eurographics Association 2010.

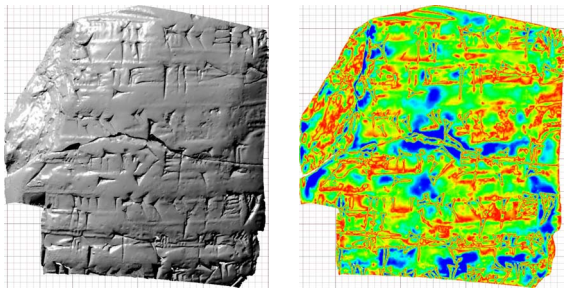

(a) (b)

Figure 2: *Orthographic projection of one 3D scan of Inv. No. 88/677 on virtual scale paper with (a) virtual light, but without texture as it is black and shiny and (b) height difference [CRS01] to a strongly smoothed surface.*

for cuneiform tablets is shown in [AL02], where spheres are fit onto the surface, which trace the wedges like a virtual stylus. The benefit of using spheres of different sizes (scales) instead of one rectangular structure representing a real stylus is its invariance to rotation. However, there is no conclusion about performance; nor about scripts of lower quality; nor any segmentation of the surface despite the achieved displacement map shows a satisfying result for visual autopsy. As we experienced drawbacks in segmentation of distorted surfaces for pottery fragments in our previous projects, a hypothesis is that curvature estimation using differential geometry [Sto69] might be the problem. In contrast one can argue that it is widely successfully applied, computationally fast and robust. This is true for industry grade objects with distinct features like rectangular edges, where often the comparison with a synthetic 3D model is possible. [HFG*06, PWHY09] demonstrates for acquired 3D models of fractured objects with arbitrary shaped features the predominance of integral invariants over methods of differential geometry.

3.1. Feature Estimation

The consequent step was to adopt the integral invariant method as *Multi Scale Integral Invariant* (MSII) filtering for extracting cuneiform characters. The principle of this approach is to intersect the volume below the surface with the volume of multiple spheres. Normalizing the volume descriptor [PWHY09] $V_{r_j}(\mathbf{p}_i)$ by $4(\pi {r_j}^3)/3$ for all spheres defined by r_j centered about all points $\mathbf{p}_i = (x_i, y_i, z_i)^T$ of the surface enables a local classification into convex ($V'_{r_j}(\mathbf{p}_i) < 0.5$), concave ($V'_{r_j}(\mathbf{p}_i) > 0.5$) and plane areas ($V'_{r_j}(\mathbf{p}_i) = 0.5$). Having concentric spheres in multiple scales we get a discrete, real-valued feature function – shortly called *feature vector* $\mathfrak{f}_i = f(\mathbf{p}_i)$. Let n be the number of scales and let $\mathcal{M}_2$ be the surface of a 3D model:

$$\begin{aligned} \mathfrak{f} : \mathcal{M}_2 &\longrightarrow]0,1[^n \\ \mathbf{p}_i &\longmapsto \mathfrak{f}(\mathbf{p}_i) = (v_1, \ldots, v_n)^T \end{aligned} \tag{1}$$

with $v_j = V'_{r_j}(\mathbf{p}_i) = \frac{3V_{r_j}}{4\pi r_j^3}$ for $1 \leq j \leq n$. We get:

$$\mathfrak{f}_i = (\, v_1, \ldots, v_n \,)^T = \frac{3}{4\pi} \left(\frac{V_{r_1}(\mathbf{p}_i)}{r_1^3}, \ldots, \frac{V_{r_n}(\mathbf{p}_i)}{r_n^3} \right)^T \tag{2}$$

Figure 3 shows an example for a vertex ($i = 25562$) on a plane part of a cuneiform tablet and for a vertex ($i = 141142$) right at the bottom of a wedge. For uniformly spread radii $r_1 = 0.2\,mm < r_2 \ldots < r_{n=5} = 1.0\,mm$ the respective *feature vectors* compute to:

$$\begin{aligned} \mathfrak{f}_{25562} &= (\, 0.499,\ 0.499,\ 0.498,\ 0.498,\ 0.498 \,)^T \\ \mathfrak{f}_{141142} &= (\, 0.578,\ 0.644,\ 0.710,\ 0.750,\ 0.732 \,)^T \end{aligned}$$

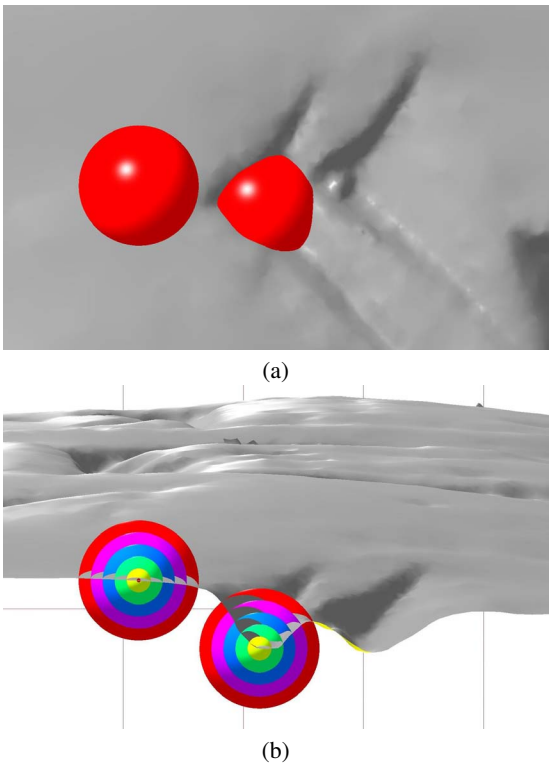

(a) (b)

Figure 3: *Magnification of a 4.5×2.8 mm area of the 3D model of Inv. No. 88/677 showing two multiscale spheres (a) from the top and (b) an intersected side view with scale paper in mm. For demonstration purpose only 5 radii are used.*

As expected the *feature vector* for the planar area shows values slightly lower than 0.5, which corresponds to the general curvature of tablets. The elements v_j of the *feature vector* within the wedge are expected to be ≈ 0.75, because the larger part of the volumes of the concentric spheres lie below the surface. The smaller the radius r_j the closer the volumes get to 0.5 – in other words, the precentage of the volumes

© The Eurographics Association 2010.

below the surface converges to 50%. This is due to the accumulated imprecision of the surface, caused by a worn-out stylus, dirt and measuring errors.

Figure 3 shows the principle visually. The volume estimation of $V_r(\mathbf{p}_i)$ and its intersection with the spheres is achieved by transforming mesh and sphere into a volume based representation using voxels instead of the surface representation by vertices and faces. The benefit of this transformation is that it can be used in a modular manner, so that the voxel filter mask for the sphere can be easily changed to a non-invariant (anisotropic [PM90]) filter. In similar manner any kind of surface representation can be quantized into voxels and simply intersected by boolean operation with any kind of filter mask. Despite anisotropy in scale-space is always an interesting method for segmentation, we choose to investigate further into the isotropic filtering using spheres due to performance reasons.

The treatment of surface borders as measured surfaces have discontinuities – shortly called holes – and require an anisotropic filtering. In case the marching front [NK02] for triangle selection within a sphere hits a border introduced by a hole, the sphere volume used for normalization is decremented by an estimated ratio between the existing surface and a planar filled hole.

Planar filling is the fastest method and heuristics have shown that the error of planar filling in contrast to more sophisticated methods is lower than errors in measurement near holes. As the single 3D scan from Figure 2a has sevearll small holes and the border of the visualization is the actual border of the 3D scan, $\approx 15\%$ (using $r_n = 1.5\ mm$) of the surface would have been ignored or faulty when border treatment would have been skipped or done incorrectly. Figure 4 using the same data as Figure 2a shows that the feature vectors are correctly determined for the whole surface.

Performance is a crucial issue as MSII done by the textbook is computationally extensive, which we overcome by designing the filtering in voxel representation using sparse matrices [Tew73] and using a filter size (in *byte*) smaller than the CPUs cache as well as using parallel processing with *POSIX*-threads [But97]. The result was a dramatic gain in performance far beyond what one expects in regard to Amdahl's law [Amd67].

Choosing the right parameters – especially r_n – influences performance as the marching front has $O(r_n log(r_n))$ to $O(r_n^2)$ complexity. [PWHY09] and [AL02] suggest to choose a certain percentage of the bounding box of the model size, which contradicts the Shannon Theorem [Sha48] for character extraction. This theorem also tells us that we have to set the sphere diameter ($2r_n$) to more than half of the wedge size to determine its outlining edges. In short terms: r_n has to be slightly larger than the largest wedge width found on a tablet. The number n of scales mostly influences memory usage and not performance. Similar is valid for the voxel space, which has to fit into the CPU cache. On recent computer hardware having a 2.8 GHz CPU and more than 8 GB of RAM, $n = 10$ and a sparse voxel space of 256^3 has proven to be a good choice.

3.2. Character Extraction

Having *feature vectors* for all vertices describing the surface, the next step is to decide which vertices belong to characters. When we interpret the *feature vectors* as points in an n-dimensional space a classification can be done by their *feature distances* $\Delta \mathfrak{f}_i = |\mathfrak{f}_i - \mathfrak{f}_k|$ using the arbitrarily chosen vertex ($k = 141142$) on the bottom of a wegde. Then histogram equalized gray values are mapped to the surface vertices $\mathbf{p}_i$ – shown in Figure 4a. Finding a threshold to use $\Delta \mathfrak{f}_i$ for segmentation is not trivial for a wider range of cuneiform script variations as well as it is not very user-friendly when it has to be set manually.

Looking at our *feature vectors* as a function (or signal) depending on r_j, a classification in Fourier space using *Fast Fourier Transform* (FFT) can be applied as done in signal processing. FFT is used in many applications – e.g. it is used in [PWHY09] in an approach to estimate surface integral invariants. The result of the FFT applied to a *feature vector* is another vector, which has no satisfying result for segmentation by thresholding in similar manner as segmentation of the *feature vectors* themselves.

An alternative to segmentation by thresholding is e.g. the use of neural networks. [Ros97] proposed this kind of classification for holographic (raster) images. As neural networks are known to perform well for small tasks, but are difficult to configure and train for complex tasks we did not investigate them any further. More interesting is the classification of the border sum of tiles of raster images using correlation in [Ros97] as it is also used in *Optical Character Recognition* (OCR) in general and for cuneiform script [AL02]. The application of cross-correlation to the *feature vectors* by convolution $(\mathfrak{f}_i * \mathfrak{f}_k)$ using the arbitrarily chosen vertex ($k = 141142$) is shown in Figure 4b, where dark colors mean high correlation. Additionally we experimented with different color scales to visualize other surface features in detail (e.g. fingerprints or seal impressions).

Investigating into correlation, FFT and signal processing moved our focus on autocorrelation [Bra65], which does not require any arbitrarily chosen vertex. The autocorrelation function R_{ff} for a continous function f is the convolution with the complex conjugate $\bar{f}$:

$$R_{ff} = f * \bar{f} = \int_{-\infty}^{+\infty} f(\tau)\bar{f}(\tau - t)d\tau = \int_{-\infty}^{+\infty} \bar{f}(\tau)f(\tau + t)d\tau \tag{3}$$

© The Eurographics Association 2010.

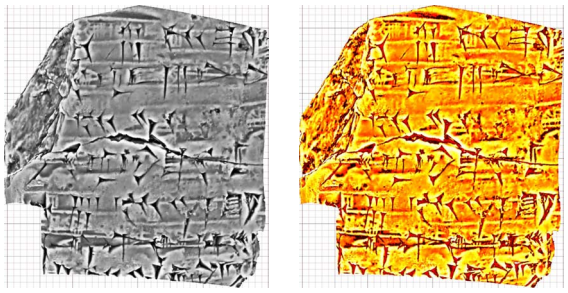

(a) (b)

Figure 4: *Inv. No. 88/677 with topological texture map calculated by (a) distance and (b) correlation to one selected feature vector representative for a wedge. Both visualization are rendered without any virtual light source.*

As our *feature vectors* $\mathfrak{f}_i = f$ are real, we can substitute $\bar{f}$ by f, and as $\mathfrak{f}_i$ is discrete, we can continue to interpret $\mathfrak{f}_i$ as a discrete signal convoluted by itself:

$$R_i = \sum_l \mathbf{R}_i(l) \text{ with } \mathbf{R}_i(l) = (\mathfrak{f}_i * \mathfrak{f}_i)(l) = \sum_{j\in\mathbb{Z}} v_j v_{l-j} \quad \text{with } v_j \equiv 0 \text{ for } j \leq 1 \wedge j \geq n \tag{4}$$

$\mathbf{R}_i(l)$ has $2n$ non-zero elements for n even and $2n-1$ non-zero elements for n odd. $\mathbf{R}_i(l)$ in Equation 4 means that the *feature vector* is understood as signal extended with zeros to both directions. The signal

$$\ldots, 0, 0, 0, v_1, \ldots, v_n, 0, 0, 0, \ldots$$

is convoluted with itself:

$$\begin{array}{c} \ldots, v_1, \ldots, v_n, 0, 0, 0, 0, 0, 0, \ldots \\ \ldots \\ \ldots, 0, 0, v_1, \ldots, v_n, 0, 0, 0, 0, \ldots \\ \ldots, 0, 0, 0, v_1, \ldots, v_n, 0, 0, 0, \ldots \\ \ldots, 0, 0, 0, 0, v_1, \ldots, v_n, 0, 0, \ldots \\ \ldots \\ \ldots, 0, 0, 0, 0, 0, 0, v_1, \ldots, v_n, \ldots \end{array}$$

Let R_i indicate the autocorrelation of the signal: Small values of R_i are located at inflection points and are shown as dark colors in Figure 5b. They mark the borders of the wedges as contour lines. Figure 5b also shows that vertices outside the contour lines can have the same autocorrelation as the vertices inside the wedges. The automatic decision, which vertices belong to wedges, is based on local minima of $\mathcal{M}_2$, which are shown in Figure 5c as bright spots. The local minima are used as seed vertices for labeling having the contour lines as stop criteria. The label borders equaling the wedge outlines are then extracted as closed polygonal lines from $\mathcal{M}_2$ for further processing as a vectorized, scaleable drawing. Such a reduction from surfaces having typically 10 to 50 million vertices to a vector representation having a few thousand vertices enables new means of OCR using 3D models – instead of using raster images. Figure 5a shows the 3D model with the acquired color of the tablet having the same illumination as Figure 5b,c.

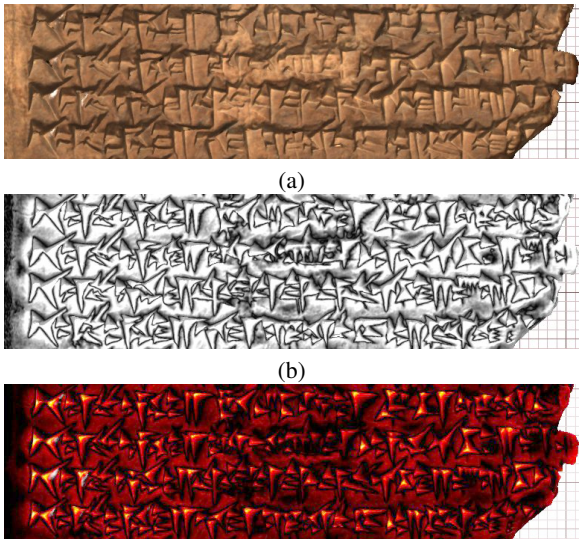

(a) (b) (c)

Figure 5: *Four lines with Omina from the shaded 3D model W20430,101,* Uruka-Warka Sammlung *(a) with acquired texture map, (b) with contourlines and (c) with local minima.*

4. Results

For first experiments we choose 25 cuneiform tablets and two clay nails with credit of donations in cuneiform script. The selection was done to test the robustness of the proposed method in contrast to the typical corpora publications. The objects acquired vary in cuneiform script over different millennia; languages; originals and copies made of different materials (ceramic and gypsum casts).

While the previous Figures show objects of rather high quality, Figure 6 is a common example including all the hassele one can expect: bad handwriting; corroded and worn-out surface; writings around the edges; strongly curved front face, which is difficult to illuminate. Additionally it is a cast copy with cast flashs and air pockets. Nevertheless, we were able to automatically extract the same amount of characters as shown in the manual autography. Figure 8 is another example for an object which is difficult to read, draw and photograph. It also demonstrates the various possibilities to visualize 3D models, while our focus otherwise is on character extraction. Rendering orthographic true to scale views from all six sides – also called *fat cross* by the CDLI – can be done as well as rollouts of clay nails.

© The Eurographics Association 2010.

(a) (b)

Figure 6: *A representative tablet of assyriologists' daily work: Cast copy of the heavily eroded tablet TCH.92,G.127. For manual autography and transciption see [Jak09]. (a) Photograph and (b) 3D model with contour lines.*

On a tablet used to train scribes in ancient times, we could also visualize fingerprints using the smallest volume descriptor v_1. This can be done even faster than extracting the characters as it does not require multiple scales: ridges of fingerprints always come in the same size. Figure 7 shows v_1 mapped as grayscale for the whole tablet and in detail for one fingerprint.

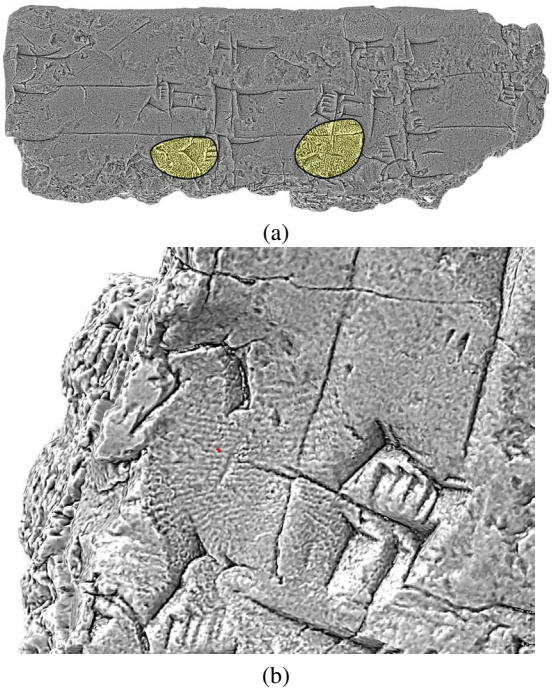

(a)

(b)

Figure 7: *True to scale visualization of Inv. No. W20248,10,* Urku-Warka Sammlung *showing two fingerprints using the topographic texture of the smallest scale. (a) Front view without illumination. (b) Detail of the right fingerprint enhanced by illumination.*

5. Summary

Summarizing the results, we could show that using state-of-the-art 3D technology in conjunction with *GigaMesh* provides a robust and fast workflow for a wide range of cuneiform tablets – especially those which are difficult to process manually. The working time using the 3D scanner including post-processing (e.g. using *Breuckmann OPTOCAT*) of the 3D scans is less than for manual drawing. Having a highly automated method for character extraction with just one, simple parameter to be set when the post-processing of the 3D model is finished, our system needs a few minutes of offline computing time depending on the resoltion (FOV) used for acquisition as well as the size of a tablet. Common and free file formats are supported (e.g. *Stanford* PLY, *Wavefront* OBJ and *W3C* VRML).

6. Outlook

Future work will use the extracted polygonal representation of cuneiform characters for character (en)coding and further data reduction, which will enable a smoother scaling of characters, e.g. by fitting splines [Sch07]. This will also simplify the integration into the CDLI, which aims to enable virtual access to all major cuneiform collections via the internet. A precise, but compressed representation of extracted characters will allow fast access e.g. for stylistic analysis, while scholars rarely will have to inspect a 3D model in highest resolution.

As 3D models acquired with the 35 and 60 *mm* FOV are interesting for research regarding traces from the stylus or seals, they also require tremendous amounts of off-line computing time, which will be improved by making more efficent use of modern hardware like using Graphics Processing Units (GPUs). For our future work we will utilize *nVidia Compute Unified Device Architecture* (CUDA) or the recently evolved *Open Computing Language* (OpenCL) as it was done for analysing chalkings of inscriptions [MHK09].

Acknowledgement

We thank Prof. Willi Jäger, Prof. Stefan M. Maul, Prof. Markus Hilgert and the *Deutsches Archäologisches Institut* (DAI) for their support and granting access to the collections of the *Assyriologie* and the *Uruk-Warka Sammlung* in Heidelberg. The 3D scanners used for this work were provided by the *Heidelberger Akademie der Wissenschaften* (HAW) and the *Heidelberg Graduate School of Mathematical and Computational Methods for the Sciences* (HGS MathComp). This work is part of the *IWR Pioneering Projects* (IPP) and partially funded by the HGS MathComp – DFG Graduate School 220.

References

[AL02] ANDERSON S. E., LEVOY M.: Unwrapping and Visualizing Cuneiform Tablets. *IEEE Computer Graphics and Applications 22*, 6 (November/December 2002), 82–88. 3, 4

© The Eurographics Association 2010.

[Amd67] AMDAHL G. M.: Validity of the Single Processor Approach to Achieving Large-Scale Computing Capabilities. In *Proc. of AFIPS Spring joint Computer Conference* (1967), vol. 30, pp. 483–485. 4

[Bra65] BRACEWELL R.: *The Fourier Transform and Its Applications*. 1965, ch. The Autocorrelation Function, pp. 40–45. 4

[Bun05] BUNNELL M.: *GPU Gems 2*. Addison Wesley, 2005, ch. Dynamic Ambient Occlusion and Indirect Lighting, pp. 223–233. 2

[But97] BUTENHOF D. R.: *Programming with POSIX Threads*. Addison-Wesley Longman Publishing Co., Inc., Boston, MA, USA, 1997. 4

[CRS01] CIGNONI P., ROCCHINI C., SCOPIGNO R.: Metro: Measuring Error on Simplified Surfaces. *Computer Graphics Forum 17*, 2 (2001), 167–174. 2, 3

[DKK*02] DEMOLI N., KAMPS J., KRÜGER S., GRUBER H., WERNICKE G.: Recognition of Cuneiform Inscription Signs by use of a Hybrid-Optoelectronic Correlator Device. *Applied Optics 41*, 23 (2002), 4762–4774. 2

[Feu00] FEUERHERM K.: The Computer Representation of Cuneiform: Towards the Development of a Character Code. Univ. of Birmingham, 2000. Listed as publication of the CLDI related to the Initiative for Cuneiform Encoding (ICE) Workshop. 1, 2

[GWLU05] GRONEBERG B., WEIERSHÄUSER F., LINNEMANN T., ULLRICH D.: *Jahrbuch der Max-Planck-Gesellschaft*. Gesellschaft für wissenschaftliche Datenverarbeitung mbH, Göttingen, Germany, 2005, ch. Digitale Keilschriftbibliothek Lexikalischer Listen aus Assur. 2

[HFG*06] HUANG Q.-X., FLÖRY S., GELFAND N., HOFER M., POTTMANN H.: Reassembling Fractured Objects by Geometric Matching. In *Proc. of Int. Conference on Computer Graphics and Interactive Technique (SIGGRAPH)* (Boston, MA, USA, 2006), ACM, pp. 569–578. 3

[Hil08] HILGERT M.: Cuneiform Texts in the Collection of St. Martin Archabbey Beuron. *Cuneiform Digital Library Journal (CDLJ) 2* (2008), online. 2

[Jak09] JAKOB S.: *Die mittelassyrischen Texte aus Tell Chuera in Nordost-Syrien*, 1 ed. Harrassowitz, O., Wiesbaden, Germany, July 2009. Tafel 26. 6

[KMT08] KALASEK R., MARA H., TAEUBER H.: Reading Weathered Ancient Laws in 3rd Dimension. In *13. Int. Tagung: Kulturelles Erbe und Neue Technologien* (Vienna, Austria, November 2008). 1

[Mau05] MAUL S. M.: *Das Gilgamesch-Epos*, 3 ed. C.H.Beck, Munich, Germany, 2005. 1

[MBLA09] MARA H., BREUCKMANN B., LANG-AUINGER C.: Multi-Spectral High-Resolution 3D-Acquisition for Rapid Archaeological Documentation and Analysis. In *Proc. of 17th European Signal Processing Conference (EUSIPCO 09)* (Glasgow, Scotland, United Kingdom, 2009), pp. 1205–1209. 1, 2

[MHK09] MARA H., HERING J., KRÖMKER S.: GPU based Optical Character Transcription for Ancient Inscription Recognition. In *Proc. of 15th Int. Conference on Virtual Systems and Multimedia (VSMM) – "Vision or Reality? Computer Technology and Science in Art, Cultural Heritage, Entertainment and Education"* (Vienna, Austria, September 2009), pp. 154–159. 1, 6

[NDE91] NISSEN H. J., DAMEROW P., ENGLUND R. K.: *Frühe Schrift und Techniken der Wirtschaftsverwaltung im alten Vorderen Orient*, 2 ed. Franzbecker, 1991, p. 200. Fig. 19. 1

[NK02] NOVOTNI M., KLEIN R.: Computing Geodesic Distances on Triangular Meshes. In *Proc. of 10th Int. Conference in Central Europe on Computer Graphics, Visualization and Computer Vision (WSCG)* (2002), pp. 341–347. 4

[PM90] PERONA P., MALIK J.: Scale-Space and Edge Detection Using Anisotropic Diffusion. *IEEE Transactions on Pattern Analysis and Machine Intelligence 12*, 7 (July 1990), 629–639. 4

[PWHY09] POTTMANN H., WALLNER J., HUANG Q.-X., YANG Y.-L.: Integral Invariants for Robust Geometry Processing. *Computer Aided Geometric Design 26*, 1 (Jannuary 2009), 37–60. 3, 4

[QTK*09] QUATEMBER U., THUSWALDNER B., KALASEK R., BATHOW C., BREUCKMANN B.: The Virtual and Physical Reconstruction of the Octagon and Hadrian's Temple in Ephesus. In *Proc. 2nd Workshop on Scientific Computing for Cultural Heritage (SCCH)* (Heidelberg, Germany, 2009), Bock H. G., Jäger W., Mara H., Winckler M., (Eds.), Springer, p. in print. 2

[Ros97] ROSHOP A.: *Digitale Mustererkennung an holographischen Bildern von Keilschrifttafeln*. Physik. Herbert Utz Verlag, 1997. Phd Thesis. 2, 4

[Sch07] SCHUMAKER L. L.: *Spline Functions: Basic Theory*, 3 ed. Cambridge Mathematical Library, Vanderbilt University, Tennessee, TN, USA, 2007. 6

[Sha48] SHANNON C.: A Mathematical Theory of Communication. *Bell System Technical Journal 27* (July and October 1948), 379–423 and 623–656. 4

[SM92] SABLATNIG R., MENARD C.: Stereo and Structured Light as Acquisition Methods in the Field of Archaeology. In *Mustererkennung '92, 14. DAGM-Symposium Dresden* (1992), Fuchs S., Hoffmann R., (Eds.), Springer, pp. 398–404. 2

[Sto69] STOKER J. J.: *Differential Geometry*, vol. 20 of *Pure and applied mathematics*. Wiley-Interscience, New York, NY, USA, 1969. 3

[Tew73] TEWARSON R. P.: *Sparse Matrices*, vol. 99. Elsevier, 1973. 4

[Uni06] UNICODE CONSORTIUM: *The Unicode Standard, Version 5.0*, 5 ed. Addison-Wesley, Boston, MA, USA, 2006. 2

[vBVD*94] VON BALLY G., VUKICEVIC D., DEMOLI N., BJELKHAGEN H., WERNICKE G., DAHMS U., GRUBER H., SOMMERFELD W.: Holography and Holographic Pattern Recognition for Preservation and Evaluation of Cultural-Historic Sources. *Biomedical & Life Sciences 81*, 12 (1994), 563–565. 2

[vS94] VON SODEN W.: *The ancient Orient: an introduction to the study of the ancient Near East*. Wm. B. Eerdmans Publishing Co., 1994. 1

[Wei10] WEIERSHÄUSER F.: Die Online-Datenbank der lexikalischen Texte aus Assur. *Mitteilungen der Deutschen Orient-Gesellschaft zu Berlin (MDOG)* (2010), in print. 2

[WGD*98] WERNICKE G. K., GRUBER H., DEMOLI N., SENONER M., VON BALLY G., DREESEN F., ROSHOP A.: Applications of Color Holography in the Investigation of Handwritten Cultural Historic Sources. In *Proc. of SPIE:: 6th Int. Symposium on Display Holography* (Lake Forest, IL, USA, July 1998), vol. 3358, SPIE – Int. Society for Optical Engineering. 2

[WS03] WATKINS, JR. L., SNYDER D. A.: The Digital Hammurabi Project. In *Proc. of Museums and the Web* (Charlotte, NC, USA, 2003), Toronto: Archives & Museum Informatics, pp. CD–ROM, Online. 2

[WTN*02] WOOLLEY S. I., T.R.DAVIS, N.J.FLOWERS, DUTOI J., A.LIVINGSTONE, T.N.ARVANITIS: Communicating Cuneiform: The Evolution of a Multimedia Cuneiform Database. *The Journal of Visible Language 36*, 3 (2002), 308–324. 2

© The Eurographics Association 2010.

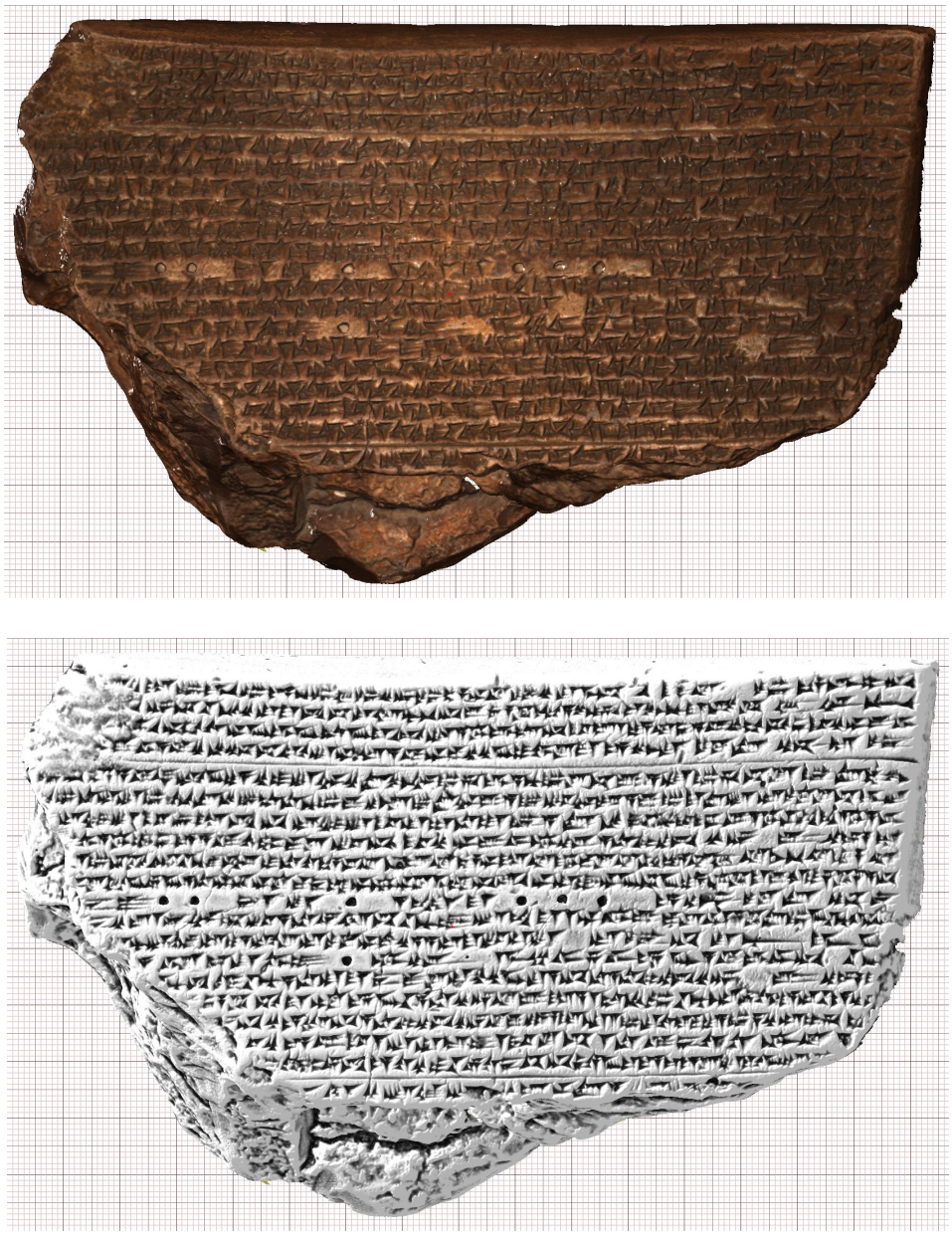

Figure 8: *True to scale (1:3/4) orthograpic projections of the 3D model of Inv. No. W51617 of the* Assyriologie Heidelberg *collection. The acquired tablet is a ceramic cast copy having a dark red, shiny surface similar to the Roman* Terra Sigillata*. From a technical point of view this 3D model contains most measuring errors as dark and shiny surfaces have adverse reflexion properties for acqusition using any kind of light source. Additionally it also adds deformation from casting and calcination, typically resulting in smoother edges of the wedges. A virtual scale paper with a mm raster is shown in the background.*
Top: Visualization of the acquired texture map illuminated by two light sources located above the top-left corner of the tablet.
Bottom: Visualization using a texture map, where the labled wedges, lines and fractures are colored in black. Additionally one light source on the top-left was used to reduce the hard contrast from the black and white labeled image for the human reader.

© The Eurographics Association 2010.